Constructive Modification of Conducting Polyaniline Characteristics in Unusual Proportion Through Nanomaterial Blend Formation with the Neutral Polymer Poly(vinyl pyrrolidone)

E. Subramanian, G. Anitha, N. Vijayakumar*

Department of Chemistry, Manonmaniam Sundaranar University Abishekapatti, Tirunelveli 627 012, Tamil Nadu, India

Received 25 July 2005; accepted 7 March 2007
DOI 10.1002/app.26566
Published online 27 June 2007 in Wiley InterScience (www.interscience.wiley.com).

ABSTRACT: The present work reports an investigation on the modification of conducting polyaniline (PANI) characteristics favorably on blending with the neutral polymer, poly(vinyl pyrrolidone) (PVP) in a systematic variation of their molar ratios (aniline : PVP = 4 : 1, 2 : 1, 1 : 1, 1 : 2, and 1 : 3). Prepared by precipitation technique by conventional *in situ* chemical oxidative polymerization with ammonium peroxodisulfate in aqueous H_2SO_4 medium (pH 1.0), these materials have nanometer sizes ($\sim$ 50–200 nm) and, depending on the molar ratios, exhibit a distinct deviation in physicochemical characteristics from those of pristine PANI prepared in the identical condition. A gradual trend in characteristics is noticed in first three PANI–PVP blends, while an abnormal hike in conductivity, unusual spectral features in IR and UV–vis, hardened nature, and induction of characteristic morphology, crystallinity, and thermal stability are associated with the last two blends that have excess PVP. Thus a division of two sets of nanoblends, one set with less or equal content of PVP and another with excess of PVP, emerges. Evidently, PVP has a tuning effect on PANI through its dopant, supporting matrix and interpenetrating steric stabilizer acts in proportion quite unusual to its neutral nature. The study altogether brings to light a simple way of modification of PANI characteristics by conventional method of blend synthesis. © 2007 Wiley Periodicals, Inc. J Appl Polym Sci 106: 673–683, 2007

Key words: polyaniline–poly(vinyl pyrrolidone) blend; codopant; nanomaterials; characteristics modification

INTRODUCTION

Polyaniline (PANI) nowadays has been receiving a wide attention because of its attractive electrical and optical properties as well as its good environmental stability that give rise to an enormous potential for versatile technological applications. However, the mechanical and processability properties of PANI are not as sufficient as desired for many of its applications. In an attempt to augment these properties, in recent years, the synthesis of PANI is redirected towards blends,[1,2] composites,[3,4] and copolymers[5] with common insulating polymers. While blending PANI with a bulk polymer carrying an anionic group like sulfonate/carbonate, it is likely that it could act as polymeric dopant/codopant and could, thus, enhance the conductivity of PANI and other properties depending on its chemical nature. Polymeric dopants are superior to conventional small-sized dopants like Cl^-, SO_4^{2-}, etc., because the former could significantly improve the stability and many of the properties of the resulting blend, but the small-sized dopant usually tends to migrate out of the polymer matrix. Most success has been achieved with PANI in the presence of other polymers, for example, poly(styrene sulfonate)[6] and poly (acrylic acid).[7] In this regard, it is emphasizable that the method of preparation and composition of blend/composite play a major role in obtaining conducting polymers with wonderful properties. For example, blending of polystyrene–polybutadiene–polystyrene thermally with not more than 20 wt % of PANI has resulted in an electrically conducting composite with a good level of conductivity.[8] Rao et al.[9] have synthesized PANI and its blends containing various percentage of polycarbonate by two different methods. Among them, the blend prepared by emulsion method with 50 wt % loading of polycarbonate has conductivity equal to that of PANI.

In this context, the water soluble polymer, poly(vinyl pyrrolidone) (PVP), is of special interest. PVP has been reported to be an effective steric stabilizer in the dispersion polymerization of pyrrole[10] and

**Present address:* Department of Physics, Sri K.G.S. Arts College, Srivaikuntam 628 619, Tamil Nadu, India.
Correspondence to: E. Subramanian (smanian2002@yahoo.com).

Journal of Applied Polymer Science, Vol. 106, 673–683 (2007)

TABLE I
Synthesis Conditions for PAPVP Blends

Sample code	Stoichiometric molar ratio (ANI : PVP)	Base mole concentration of PVP (*M*)	Volume of PVP (mL)	Volume of water (mL)
PAPVP1	4 : 1	0.2	25	55
PAPVP2	2 : 1	0.4	25	55
PAPVP3	1 : 1	0.5	40	40
PAPVP4	1 : 2	0.5	80	–
PAPVP5	1 : 3	0.75	80	–

Total volume = 100 mL; Volume of 1.0*M* aniline = 20 mL.

aniline.[11–14] Ghosh et al.[11] have synthesized PANI–PVP blend finely-dispersed in aqueous medium, with a 10% PVP solution and an equimolar aniline (ANI) and ammonium peroxodisulfate (APS) (5.5×10^{-4} to 5.5×10^{-3} mol) solution. In our previous study,[15] we have observed that PVP could act as a polymeric codopant along with the sulfate counter ion and the phenomenon that is quite unexpected for a neutral polymer was established with the PANI–PVP blend of 2 : 1*M* ratio synthesized by precipitation method at room temperature. Even with an amount equal to half of PANI, PVP in this blend has witnessed many constructive roles including the codopant activity. Hence it is interesting to investigate the effect of PVP in higher amounts on PANI in relation with synthesis temperature and to understand the physicochemical principles through which PVP alters the characteristics of such new blends. These aspects are essential because the synthesis conditions greatly affect the structure, morphology, and final properties of conducting PANI materials. Therefore, the aim of the present work is the synthesis of PANI–PVP blends (denoted as PAPVP) in various molar stoichiometric ratios (with PVP content lower, equal, and higher than PANI content) at 0°C, and a systematic study on their electrical, spectral, morphological, and thermal properties in comparison with PANI prepared in the identical condition.

EXPERIMENTAL

Materials

Aniline (SD Fine Chemical, India) was purified by distillation over zinc dust before use. PVP of average molecular weight 40,000 (99.5% purity) was from Sisco Research Laboratory, India, and was used as such. Double distilled water was used in all experiments. All other chemicals were of reagent grade and were used as such without further purification.

Synthesis of blend materials

PAPVP blend materials were prepared by *in situ* chemical oxidative precipitation polymerization method using APS as oxidant in aqueous H_2SO_4 medium pH $\sim$ 1 at 0°C. In a typical procedure, 20 mL of 1.0*M* aniline in aqueous H_2SO_4 mixed with PVP solution (volume and concentration varied according to the blend molar ratio; Table I) in double distilled water (total volume 100 mL) was stirred with a magnetic stir bar for about 1.0 h at 0°C. Aniline solution did not show any change with PVP because PVP remained as an inert polymer. But stirring ensured a complete physical interaction as evident from UV–vis spectra. Hundred milliliters of precooled 0.2*M* APS was added to ANI–PVP solution dropwise with constant stirring. (After complete addition, the molar ratio of APS/ANI would become 1.0). The reaction mixture was left 1.0 h with constant stirring and was then kept overnight in a refrigerator for the completion of polymerization. The polymer mass obtained was filtered, washed several times with distilled water and acetone until the washings were colorless, and finally with 0.1*M* H_2SO_4 and the sample was dried in an air oven at 110°C for about 7.0 h. The dried polymer sample was ground into fine powder and the yield was noted. By keeping the ratio of the aniline to the oxidant constant and varying the ratio of aniline to PVP, the blends of different compositions were synthesized.

For the purpose of comparison, PANI sulfate salt was also synthesized in the identical condition without PVP and is referred to as PANI.

Conductivity measurement

DC electrical conductivity of the freshly prepared blend materials was measured by a standard collinear four probe method at room temperature as described in literature.[16] For each material a batch of two pellets were made using a hydraulic press (KIMAYA Engineers, India, model WT-324) by applying 3 ton pressure; diameter 13 mm and thickness $\sim$ 2 mm. *I–V* values for the two pellets were recorded at different positions of the pellets by making a gentle contact with a gold-tipped collinear four probe set-up and drawing current from a constant power supply unit (Scientific Equipment and Serv-

ices, Roorkee, model DFP-02). From the slopes of the *I–V* plots that were linear and overlapping for different position measurements, the resistances were determined and the conductivities were calculated.

The variation in conductivity between the two pellets of the same material was very small. Thus the consistency in measurements was checked and the average conductivity of the two pellets was also calculated.

Density measurement

Density measurements were made[17] on two pellets of each of the PAPVP blend materials at room temperature from their thickness (l), radius (r) and mass (m) of the pellet using the formula,

$$\text{Density} = m/\pi r^2 l \quad (1)$$

where the denominator represents the volume. The average density of the two pellets was also calculated.

FTIR spectroscopy

FTIR spectra of the blend materials (in spectral grade KBr pellets) were recorded on JASCO FTIR-410 spectrophotometer provided with computer software. The recording was performed in 4000–400 cm^{-1} wave number range with a resolution of 2 cm^{-1}.

UV–vis spectroscopy

The UV–vis spectra of the blend materials in the solvents, dimethyl sulfoxide (DMSO) and *m*-cresol were obtained in the wavelength range 330–1100 nm on Perkin–Elmer spectrophotometer, Lambda 25 model, in matched 1-cm quartz cuvettes. The aliquots for UV–vis spectra were prepared by dispersing 8 mg of each polymer material in 6 mL of each solvent and allowing it to dissolve overnight. The clear supernatant polymer solution was used in the spectral measurement.

SEM characterization

Scanning electron micrograph (SEM) images of PANI and its blend materials in different magnifications were observed with Hitachi S-450 or Jeol JSM 5610LV microscope operating at 20 kV, after coating the samples with gold to a thickness of 100 Å using Hitachi HOS 5 GB vacuum evaporator or Jeol JFC 1600 auto fine coater with sputtering technique.

Structural characterization with XRD

XRD patterns for the powder blend samples were observed on Philips Analytical computer-controlled X-ray diffractometer using CuK_α radiation (λ = 1.5418 Å) scanning between angle 10° and 90° in a step of 0.1°/s, available at Indian Institute of Science, Bangalore.

Thermal characterization

Thermal studies (TGA and DTG) of PAPVP blends were carried out from 50 to 800°C under air atmosphere with a heating rate of 20°C/min with Perkin–Elmer thermogravimetric analyzer, model 7 at the Catalysis Laboratory, Indian Institute of Technology Madras, Chennai.

RESULTS AND DISCUSSION

Yield, density, and conductivity

Table II lists the yield, density, and room temperature conductivity of the freshly prepared polymer samples measured by standard collinear four probe method. The yields of PAPVP blends are higher than PANI itself. The gradual increase in yield from PAPVP1 to PAPVP5 reveals the inclusion of PVP in increasing amounts in the blend. The density of PANI (1.21 g cm^{-3}; Table II) is comparable with the already reported value of 1.26 g cm^{-3}.[17] But the density of PAPVP blends is found to be higher than that of PANI. This result explains the hard nature of PAPVP blends, against the soft PANI, observed during handling, especially during powdering, pelletizing, and aliquot preparation for spectroscopy. This is quite reasonable if one considers the interpenetration of PVP into PANI matrices. It was reported in a previous study on PANI/silica composite[18] that the incorporation of increasing amount of silica, leads to an elevation in density of PANI.

With regard to conductivity, there is a slight decrease in PAPVP1 and PAPVP2, almost equal in PAPVP3 and an abrupt increase in PAPVP4 and PAPVP5 blends i.e., an eightfold increase from PANI. Cautiously this trend was checked by repeated blend preparation and conductivity measurement and was found to be true. A possible reason could be as follows. When the PVP concentration is small, i.e., in PAPVP1 and PAPVP2 blends,

TABLE II
Yield, Density, and Conductivity of Blend Materials

Sample	Yield (g)	Density (g cm^{-3})	Conductivity (S cm^{-1}) (collinear four probe method)
PANI	1.89	1.21	5.06
PAPVP1	1.93	1.52	2.11
PAPVP2	1.95	1.29	3.57
PAPVP3	1.97	1.54	4.72
PAPVP4	2.04	1.44	40.00
PAPVP5	2.62	1.46	39.22

the overall interaction and the orientation of PVP chains within PANI domain might be incoherent and scattered such that PVP disrupts the ordered/crystalline region of PANI, causing a decrease. However, with increase in PVP concentration, this may turn to the other side and further the dopant role of PVP might become greater (partial negative charge on oxygen of PVP interacting with positive imine center of PANI[15]). Hence in 1 : 2 and 1 : 3 ratio blends, it becomes so high that an abnormal raise in conductivity is caused. Similar observations have been reported in anionic surfactant–PANI systems with an increase in yield[19] and also the conductivity[20] of the polymer. The other characteristics of PANI–PVP blends shed some light at the molecular level and provide an insight into their interactions.

IR spectral studies

Figure 1 illustrates the FTIR spectra of PANI, all the blend materials and PVP; Table III summarizes the peak positions and the features for each material. Since only two major less-significant peaks appear in the wave number region 4000–2000 cm^{-1}, spectra without this region are shown in Figure 1 but the data are included in Table III. Several reports were consulted for such peak assignment (PANI/blend,[5,21-24] SO_4^{2-},[24,25] and PVP[26]). The first strong and broad peak at 3600–3400 cm^{-1} assignable to O—H stretching occurs due to the absorbed/coordinated water of both PANI and PVP, because they have the tendency to acquire water of hydration due to the presence of hydrophilic groups. TGA data (Table V) are in confirmatory to this observation. The second multiple of peaks actually observed five in number in PANI films by Trchova et al.[22] were given the name ''H peaks'' and are assigned to the N—H and C—H stretching vibrations. The individual C—H assignments are available in Ref. 5. The other peaks listed in Table III, except those of PVP, are the commonly observed peaks for PANI.[21]

PANI characteristic peaks undergo shifting in peak position as well as intensity change on incorporation of PVP in its blend. The O—H and ''H peaks'' on addition of PVP become weak/feeble in the initial stage but get intensified at higher PVP content. On the other hand, the Q (Quinoid) and B (Benzenoid) ring stretching peaks, C—H out-of-plane bending and N—H (B ring) bending peaks initially strong become weak/feeble with greater PVP addition. The initially strong peaks of the vibrations, QN—H^+B (imine), BN—HB (secondary amine), 1,4-disubstituted ring stretching, N—H Q ring bending and S—O and S=O get further intensified with PVP. Uniquely, the conductivity peak split into two peaks, one at 1181 and another at 1069 cm^{-1} in former and at 1171 and 1064 cm^{-1} in latter blend. The 1069 and 1064 cm^{-1}

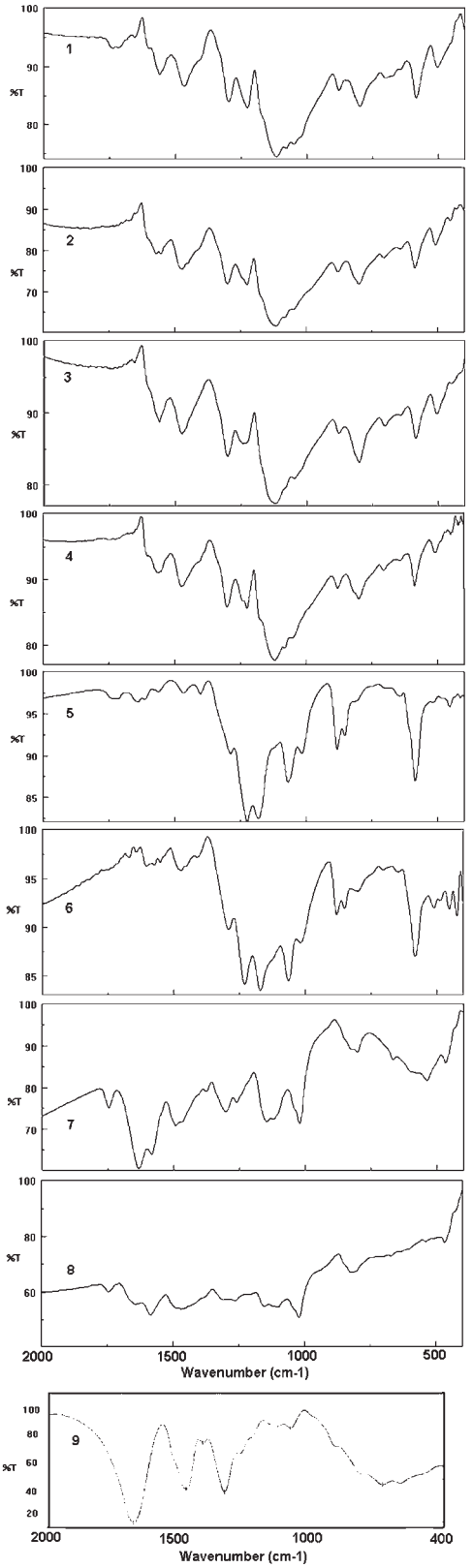

Figure 1 FTIR spectra of (1) PANI, (2) PAPVP1, (3) PAPVP2, (4) PAPVP3, (5) PAPVP4, (6) PAPVP5, (7) PAPVP3–NaOH treated, (8) PAPVP5–NaOH treated, and (9) PVP.

TABLE III
FTIR Spectral Peak Positions (cm^{-1}) and Features

Sample	O—H stretching	N—H & C—H stretching "H peaks"	Q ring stretching	B ring stretching	QN—H^+ B imine stretching	BN—HB secondary amine stretching	Conductivity peak; C—H aromatic in-plane bending	1,4 B ring disubstituted vibration	C—H aromatic out-plane bending	N—H bending Q ring	N—H bending B ring	S—O & S=O vibration	C=O stretching PVP	CH_2 deformation PVP	N—H imide stretching PVP
PANI	3600–3400, strong, broad	3100–2800, multiple with one strong peak	1559, strong	1466, strong	1297, strong	1226, strong	1115, very strong, broad	878, fairly intense	798, strong	585, strong	505, strong	1050, 1030, strong, overlapped with conductivity peak	–	–	–
PAPVP1	Weak	Feeble/ disappearing	1568, strong	1472, strong	1299, strong	1225, strong	1116, very strong, broad	878, fairly intense	799, strong	586, strong	508, strong	1050, 1030, strong, overlapped with conductivity peak	Not appearing	Not appearing	Not appearing
PAPVP2	Weak	Feeble/ disappearing	1560, strong	1474, strong	1301, strong	1236, strong	1119, very strong, broad	877, fairly intense	801, strong	586, strong	506, strong	1050, 1030, strong, overlapped with conductivity peak	Not appearing	Not appearing	Not appearing
PAPVP3	Fairly intense, broad	Fairly intense	1565, strong	1472, strong	1300, strong	1224, strong	1112, very strong, broad	880, fairly intense	799, strong	588, strong	512, strong	1050, 1030, strong, overlapped with conductivity peak	Not appearing	Not appearing	Not appearing
PAPVP4	Very strong, broad	Fairly intense	1559, weak	1464, weak	1287, strong, overlapped with $\sqrt{}_{N-H}$ imide, PVP	1224, very strong	disappeared; a new peak at 1181	882, strong doublet	800, feeble	585, very strong	512, feeble	1069, very strong separate peak without overlapping	1638, weak	1401, weak	1287, strong, overlapped with $\sqrt{}_{N-H}$ secondary amine
PAPVP5	Very strong, very broad	Fairly intense	1551, weak	1473, week	1291, strong, overlapped with $\sqrt{}_{N-H}$ imide, PVP	1230, very strong	disappeared; a new peak at 1171	880, strong doublet	800, feeble	582, very strong	511, week	1064, very strong, separate peak without overlapping	1603, week	1420, week	1230, strong, overlapped with $\sqrt{}_{N-H}$ secondary amine

peaks arise due to the S—O and S=O vibration. Salaneck et al.[27] observed a band at 1171 cm^{-1}, termed it an electronic-like band (correlative to high conductivity), and considered it as a measure of degree of delocalization of π electrons. In our case also, in consistent with the IR results of conductivity peak, the PAPVP4 and PAPVP5 blends exhibit an abnormal hike in conductivity (8 times) compared to other samples.

Like PANI, the blending agent PVP also has characteristic vibrational groups like C=O, C—H, and N—H.[26] But their appearance are not detectable in first three blends, may be due to the low concentration of PVP. Nonetheless, in last two blends where [PVP] > [ANI], their appearance must have been higher. But contrarily, N—H imide peak (strong) has overlapped with N—H secondary amine and the other two characteristic peaks of PVP show only a weak/feeble appearance. However, they show a considerable red-shift (from 1657 cm^{-1} for C=O and 1444 cm^{-1} for C—H in native PVP; Fig. 1 spectrum 9). These observations suggest that PVP extends its interaction (codopant, steric stabilizer, etc.,) by staying latently within PANI matrix, probably through interpenetrating ''hydrogen bond chain crosslinks.'' Conversion of emeraldine salt to emeraldine base of PAPVP3 and PAPVP5 blends (representative for lower/equimolar and higher [PVP] blends) by treatment with 1.0*N* NaOH for 1 day, adds evidence to this. A weight decrease of about 40% owing to the removal of sulfate was observed together with several orders of decrease in conductivity (immeasurably small) in these two samples (proof for codopant operation of PVP only with SO_4^{2-} ions). The IR spectra of emeraldine base samples (Fig. 1, spectra 7 and 8) reveal that the PAPVP3 (1 : 1 ratio) blend has exposed PVP (as evident from the intense carbonyl peak) after the removal of sulfate but the last blend PAPVP5 (1 : 3 ratio) still hides PVP, though exposed somewhat better in emeraldine base. Therefore, it becomes obvious that greater the amount of PVP, greater is the interaction between PANI and PVP.

The IR spectral study yields certain concrete inferences. First, the extent of spectral change is indicative of the degree of interaction between PANI and PVP, which, in turn, depends on the amount of PVP in the blend. From lower to equimolar [ANI] : [PVP] ratio, the observed spectral change is gradual and takes up one trend; but with higher PVP content, the change seems to be abnormal and follows another trend, suggesting different types/level of interaction. An earlier study has reported a similar phenomenon. Zengin et al.[28] have synthesized PANI–multiwalled carbon nanotube composite films with conductivity in the order of magnitude higher than that of PANI and interpreted the result as due to the existence of ''dopant effect'' of carbon in PANI composite.

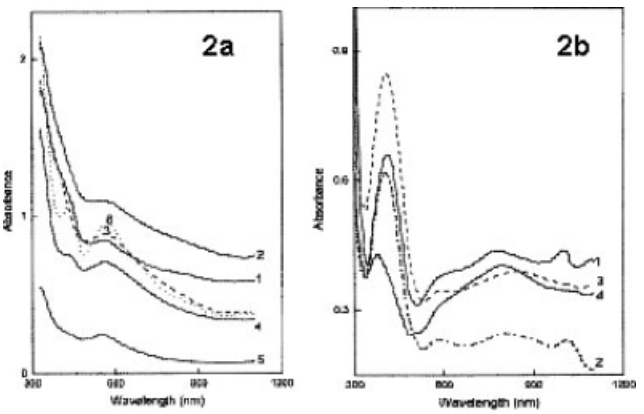

Figure 2 (a) Absorption spectra in the visible region of (1) PANI, (2) PAPVP1, (3) PAPVP2, (4) PAPVP3, and (5) PAPVP4 in DMSO. (b) Absorption spectra in the visible region of (1) PANI, (2) PAPVP1, (3) PAPVP2, and (4) PAPVP3 in *m*-cresol.

UV–Vis spectral studies

Figure 2(a,b) depicts the visible absorption spectra of the materials in DMSO and *m*-cresol solvents, respectively. In DMSO, PANI and its five blend materials exhibit unusual spectra. Initially the spectra commence with a strong absorption (absorbance ~ 2.0) at 325 nm, descend steeply, form a hump/shoulder around 550 nm and then subside gradually up to 1100 nm. Since all the materials have fine particles having nanometer sizes (~ 200 nm from SEM; Fig. 3), during overnight dispersion for aliquot preparation, DMSO being a polar solvent, might break interparticle adhesion and might form colloidal dispersion of various particle sizes. When incident light falls on aliquot, the nanoparticles of PANI/blend scatter it extensively, resulting in strong absorption in the initial stage. As the wavelength increases, the scattering diminishes, probably due to the widening difference of particle size and incident light wavelength. Anyway the scattering appears to extend up to 450 nm and in this wavelength range (325–450 nm), two characteristic peaks, π–π* (300–340 nm), and polaronic transitions (400–450 nm)[29] fall. Owing to this scattering phenomenon, displacement of peaks, especially the polaronic transition might take place, which appears as a hump/shoulder at 550 nm. Almost a similar absorption spectrum has been reported for colloidal PANI–PVA blend.[30] Since PAPVP4 and PAPVP5 blends have ''crystalline phase'' (from SEM; Fig. 3), their dispersion in DMSO is meager/nil, leading to low-intense absorption spectra.

In *m*-cresol (Fig. 2b) the spectra appear differently. PANI and its first three blends display an intense sharp peak at about 400 nm and a broad one around 800 nm. They indicate the presence of polarons and emeraldine salt, respectively.[29] However, the spectra

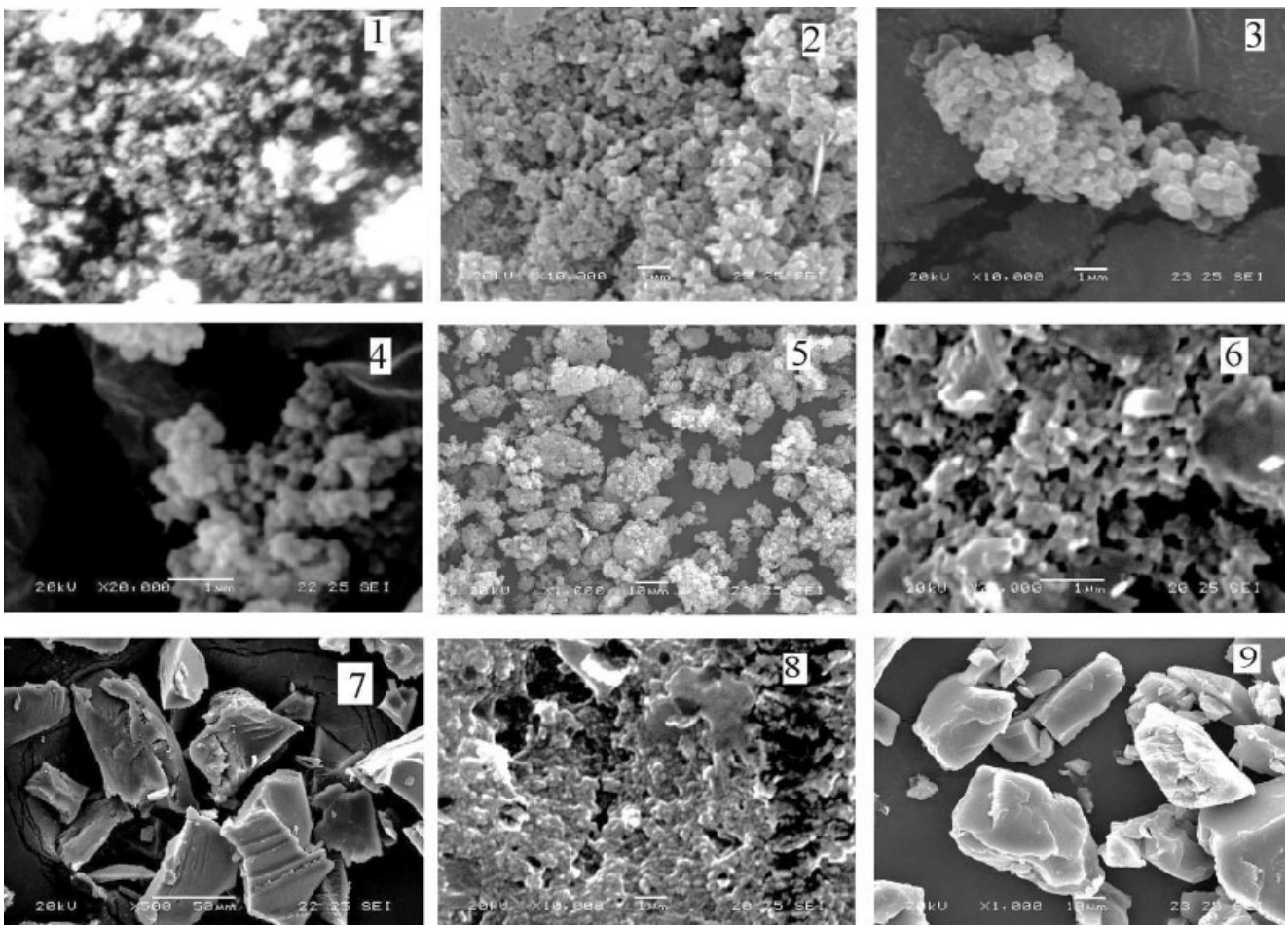

Figure 3 SEM images of (1) PANI (2000), (2) PAPVP1 (10,000), (3) PAPVP2 (10,000), (4) PAPVP3 (20,000), (5) PAPVP3 (1000), (6) PAPVP4 (20,000), (7) PAPVP4 (500), (8) PAPVP5 (10,000), and (9) PAPVP5 (1000) blend materials (times of magnification given in parenthesis next to each sample).

of PAPVP4 and PAPVP5 could not be recorded due to the poor solubility of the materials leading their absorbance to the negative region.

These spectral studies point out one clear fact that PVP does not offer any advantage to the solubility of PANI in PAPVP4 and PAPVP5. In these two cases, it was specifically observed that the particles were so dispersed in their mother liquor during synthesis (observed by Ghosh et al.[11] also), perhaps due to their nanoscale; but once carefully filtered and perfectly dried, they became compact and hardened as noticed on grinding them and were unable to disperse/dissolve. An earlier observation[31] that the insoluble part contributes to greater electrical conductivity in conducting PANI, resembles with the present observation of lower solubility and greater conductivity of PAPVP4 and PAPVP5.

SEM characterization

Figure 3 illustrates the SEM images of PANI and its five blend materials in different orders of magnification. As seen clearly from the images, PANI and its first three blend materials (PAPVP1–3) have spherical particles with a smooth homogeneous surface structure.[32] The sizes of the particles vary and an approximate size range that could be deducible on careful view is 50–200 nm. However, the particles undergo agglomeration/aggregation resulting in grains of irregular size and shape, the agglomeration being to a larger extent in PANI–PVP blends than in pristine PANI. This observation demonstrates the facilitating surface adhesion and close packing nature of blend materials.

In the case of PAPVP4 and PAPVP5 blends, the surface morphology remains distinct from others (Fig. 3, images 6–9). For these two blends the SEM images were recorded both at lower magnification (for particles after preparation) and at higher magnification (for layer of dried particles on glass slide from dispersed mother liquor of synthesis). From the higher magnification image (20,000; image 6), it appears that the dispersed PAPVP4 blend has many surface-fractured clumps/bigger aggregates, with

lesser number of individual spherical particles. However, at lower magnification (500; image 7), the same blend material presents in clear well-defined sharp ''crystalline objects.'' Similar is the case with the last blend PAPVP5 also. Perhaps, this ''crystalline phase'' may be responsible for the hardened nature of PAPVP4 and PAPVP5 blends. The unusual clump formation at higher PVP concentrations firmly suggests an interpenetrating and networking role of PVP. Up to 1 : 1*M* ratio of ANI : PVP, i.e., PAPVP3 blend, this role is minimal or marginal such that the blend materials can be segregated or dispersible as evident from the SEM picture of PAPVP3 blend (Fig. 3, image 5, 1000× magnification without any crystalline object as compared to PAPVP5 at the same magnification). Conclusively the SEM pictures together with the UV–vis spectra intensity give rise to the inference that the mother liquors of PAPVP blends contain dispersed nanoparticles and only on washing and drying process, particle agglomeration/aggregation in first three blends, and ''crystalline phase'' formation in last two blends take place. In this context the Ghosh et al.'s[11] report would be supportive. They have noticed the fine dispersion or near solution of PANI–PVP blends in aqueous mother liquor medium and have found that it was stable even for 6 months.

XRD studies

Figure 4 illustrates the XRD patterns of the polymer samples (pristine PANI, PVP, and PANI–PVP blend materials) and Table IV presents the corresponding data. It is discernible from Figure 4 that the observed peaks of all the materials are diffuse and considerably broad and they provide, by virtue of this feature, another evidence for the nanoscale materials. In comparison to PVP, that displays diffraction peaks at $2\theta = 11.66^\circ$ and 20.85°, PANI and its blends exhibit peaks at about 21° and 25°. It follows then that the first peak of PVP has no relevance in PANI–PVP blends while its second peak remains integrated with the closely lying first peak of PANI (20.75°) in the blends. A close examination of the peak positions in Table IV further reveals that peak 1 is displaced towards the higher angles (lower *d*-space), while peak 2 remains a constant for first three blends and shifts to the lower angle (higher *d*-space) in last two blends. Thus the two peaks move mutually closer. These two peaks are mainly attributable to the interchain periodicity of the polymer samples. The *d*-space for the peak at 25° is a measure of close contact distance between two adjacent PANI chains with the phenyl rings nearly located in the plane of the nitrogen atom.[33] The blend materials have lesser interchain distance between two adjacent PANI chains than is present in pristine PANI (from peak

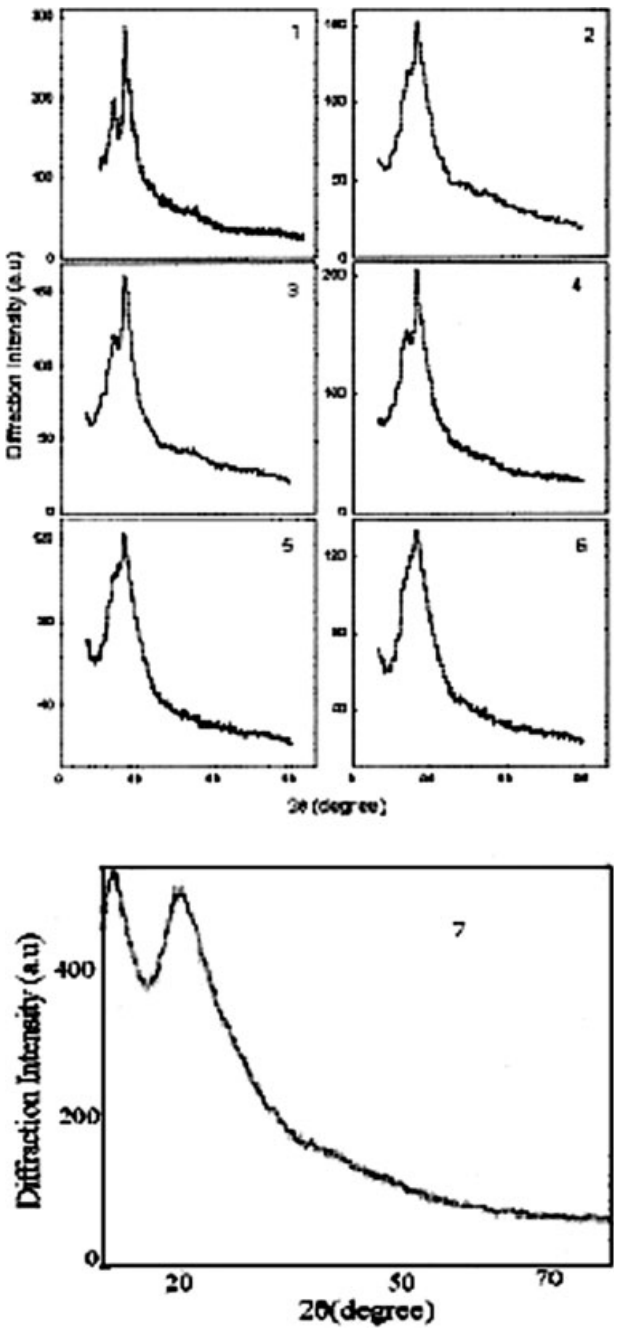

Figure 4 XRD of (1) PANI, (2) PAPVP1, (3) PAPVP2, (4) PAPVP3, (5) PAPVP4, (6) PAPVP5, and (7) PVP.

1). This suggests substantial order of crystallinity in blends than in PANI. This is explicable by the fact that the large size PVP chains establish a proximal contact with PANI chains and thereby prevent the twist of PANI chains and maintain them in more expanded conformation.[34–36] Further, as evident from the last column of Table IV, the peak intensity ratios of PAPVP1, PAPVP2, and PAPVP3 are high whereas those of PAPVP4 and PAPVP5 are low. Thus the XRD observations divide the five blend materials in to two groups and this result coincides

TABLE IV
XRD Data of Blend Materials: Peak Position (°), *d* Space (Å), and Intensity (a.u.)

	Peak 1			Peak 2			
Sample	2θ	*d* space	I_1	2θ	*d* space	I_2	I_2/I_1
PANI	20.75	4.281	201	25.02	3.560	293	1.457
PAPVP1	21.19	4.191	128	25.23	3.528	155	1.210
PAPVP2	21.59	4.114	125	25.13	3.542	167	1.336
PAPVP3	21.55	4.122	155	25.17	3.539	210	1.354
PAPVP4	22.65	3.928	111	24.63	3.616	128	1.153
PAPVP5	22.79	3.904	126	24.14	3.684	137	1.087
PVP	11.66, 20.85	7.591, 4.260	525, 494				

with all previously discussed results of conductivity, IR, UV–vis, and SEM.

Thermal studies

Thermograms of TGA are displayed in Figure 5 and the results are summarized in Table V. PANI and its blend materials undergo three-step weight losses, which correspond, respectively, to the elimination of loosely bound or mobile water molecules, removal of dopants and other small molecules from the polymer phase, and degradation of polymer itself.[37] However, for native PVP there are only two weight loss steps corresponding to water elimination and polymer decomposition, respectively. The second step, of course, consists of a steep weight loss followed by a gradual one. PANI has the highest weight loss of 18.6% in the first step indicating a large amount of absorbed water. With the inclusion of PVP in PANI, however, this weight loss decreased. For the blends it is around 8%, except for PAPVP4 where this is minimal. This shows that incorporation of PVP in PANI reduces the extent of bound water molecules and this reduction reaches maximum at PAPVP4. In the second step weight loss, PANI exhibits a higher value (34.2%) than the first three blend materials. However, PAPVP4 and PAPVP5 are exceptional by suffering the highest weight losses and also by exhibiting the highest inflection point (385°C by PAPVP5). As PVP has very high tendency to absorb moisture and anions,[38] PVP in these blends could have bound water and also the SO_4^{2-} ions. It is these species, which may eliminate largely during the second-stage degradation. In the case of first three blends, since PVP content is lesser or equal to ANI, this elimination may be nil or of lesser degree. The third step weight loss in PAPVP blends is higher than that in PANI but the extent declines with PVP content. The greater weight loss is in quite agreement with the expectation that both PVP and PANI would undergo decay at the third stage. The decrement, however, pinpoints the strengthening as well as the elevation in PANI–PVP interaction with PVP content. Supplementing this interpretation, the inflection point for the polymer decomposition is shifted to higher temperature in PAPVP4 (699°C) and it could not even be observed in PAPVP5. Also, the percentage of residue in PAPVP blends at 800°C generally increases with increase in PVP content. Thus, incorporation of PVP in PANI in excess amounts improves the amount of conducting phase and this phenomenon is not an uncommon one and it all depends on the degree of doping and the nature and amount of primary dopant (in our case SO_4^{2-} ions) present in the conducting polymer material. The largest residue for PAPVP5 clearly suggests that PVP and PANI chains are strongly interacting so as to effectively block the degradation of PANI chain. This observa-

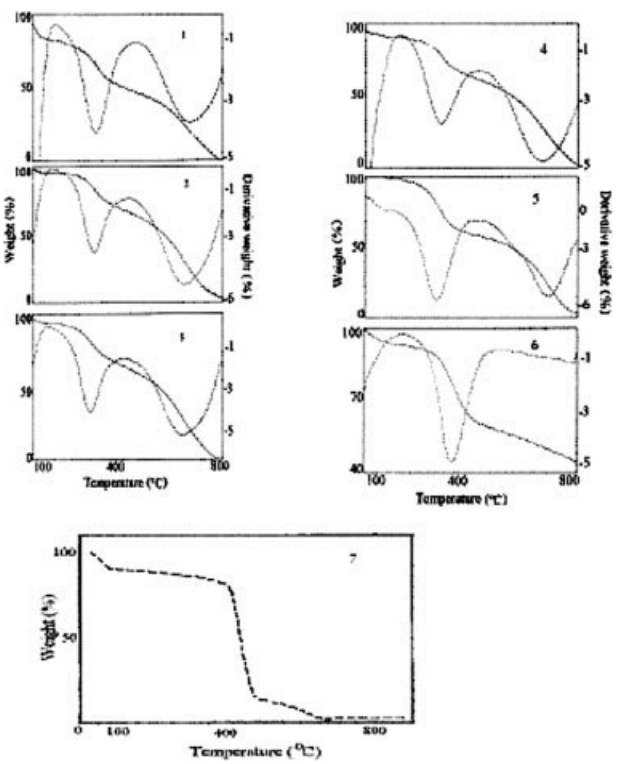

Figure 5 (—) TGA and (· · ·) DTG curves of (1) PANI, (2) PAPVP1, (3) PAPVP2, (4) PAPVP3, (5) PAPVP4, and (6) PAPVP5; (· · ·) TGA curve of (7) PVP.

TABLE V
TGA and DTG Data of Blend Materials

Sample	Temperature range (°C)	% of weight loss	% of residue at 800°C	DTG inflection points (T, °C)		Comments
PANI	Up to 150 150–450 450–788	18.6 34.2 47.2	No residue	303	670	Decomposition is completed by 788°C with one sharp and one broad inflection points
PAPVP1	Up to 167 167–435 435–800	7.9 27.2 63.0	1.9	300	658	Decomposition is not completed by 800°C with one sharp and one broad inflection points
PAPVP2	Up to 158 158–445 445–790	6.5 30.2 63.3	No residue	293	658	Decomposition is completed by 790°C with one sharp and one broad inflection points
PAPVP3	Up to 150 150–450 450–800	9.6 29.2 59.7	1.5	300	661	Decomposition is not completed by 800°C with one sharp and one broad inflection points
PAPVP4	Up to 150 150–456 456–800	1.3 39.3 54.5	4.9	303	699	Decomposition is not completed by 800°C with one sharp and one broad inflection points
PAPVP5	Up to 200 200–550 456–784	6.6 36.4 10.3	46.7	385	–	Decomposition is not completed by 784°C with one sharp inflection point
PVP	Up to 200 200–700	11.0 86.9	2.1			Decomposition is completed by 663°C with a steep weight loss during 397–477°C

tion is in perfect agreement with the previous characterization results and the corresponding interpretation of PANI–PVP chain interpenetration and ''crosslinks.'' The thermal characterization, thus, unequivocally establishes the improved thermal stability of PAPVP blends and explains the hardened nature, especially of PAPVP4 and PAPVP5 blends. Conforming to IR, UV–vis, SEM, and XRD characterizations, here also, PAPVP4 and PAPVP5 exhibit remarkably different behavior from other three blends.

CONCLUSIONS

The studies reveal that PVP acts as codopant along with SO_4^{2-} ion in all the five blend materials. Of the five, the three blend materials with PVP loading lesser than or equal to aniline concentration exhibit conductivity in increasing order with its content, while the other two blend materials with excess PVP have unusually higher conductivities than PANI. This difference in electrical property caused by the PVP content is reflected in their spectral, structural, and thermal properties also. With excess PVP content, thus, the blend materials become high-conducting, hardened, more crystalline, less-soluble, and thermally resistant. Despite the demerit of less-solubility, the introduction of PVP, a water-soluble polymer into PANI blend greatly enriches the latter's characteristics beyond expectation depending on the input molar ratios. All this is made possible through PVP's dopant, supporting matrix, and interpenetrating steric stabilizer acts in dimensions quite unusual to its neutral nature. On the whole, the study deciphers a simple way of modification of PANI characteristics in pursuant to desire through the conventional chemical route of blend synthesis with PVP.

The authors gratefully acknowledge the help rendered by Professor S. V. Subramanyam, Department of Physics, Indian Institute of Science, Bangalore, for XRD characterization.

References

1. Rao, P. S.; Sathyanarayana, D. N. J Appl Polym Sci 2002, 86, 1163.
2. Wang, Y.; Wang, X.; Li, J.; Zhang, H.; Mo, Z.; Jing, X.; Wang, F. J Polym Sci Part B: Polym Phys 2002, 40, 605.
3. Gangopadhyay, R.; De, A.; Ghosh, G. Synth Met 2001, 123, 21.
4. Chipara, M.; Hui, D.; Notingher, P. V.; Chipara, M. D.; Lau, K. T.; Sankar, J.; Panaitescu, D. Composites B 2003, 34, 637.
5. Kim, B. J.; Oh, S. G.; Han, M. G.; Im, S. S. Polymer 2002, 43, 111.
6. Ding, H.; Park S. M. J Electrochem Soc 2003, 150, E33.
7. Athawale, A. A.; Kulkarni, M. V.; Chabukswar, V. V. Mater Chem Phys 2002, 73, 106.
8. Estrada, R. H. C.; Folkes, M. J. J Mater Sci 2000, 35, 5065.
9. Rao, P. S.; Subrahmanya, S.; Sathyanarayana, D. N. Synth Met 2004, 143, 323.
10. Armes, S. P.; Aldissi, M. J Chem Soc Chem Commun 1989, 88.
11. Ghosh, P.; Siddhanta, S. K.; Chakrabarti, A. Eur Polym J 1999, 35, 699.
12. Stejskal, J; Sapurina, I. J Colloid Interf Sci 2004, 274, 489.
13. Sulimenko, T.; Stejskal, J.; Krivka, I.; Prokes, J. Eur Polym J 2001, 37, 219.
14. Somani, P. R. Mater Chem Phys 2002, 77, 81.
15. Murugesan, R.; Anitha, G.; Subramanian, E. Mater Chem Phys 2004, 85, 184.
16. Wieder, H. H. Laboratory Notes on Electrical and Galvanomagnetic Measurements; Elsevier: Amsterdam, 1979; Chapter 1, p 17.
17. Ram, M. S.; Palaniappan, S. J Mol Catal A 2003, 201, 289.
18. Chowdhury, A. N.; Rahman, J. M. A.; Rahman, M. A. Indian J Chem 2002, 41A, 1789.
19. Stejskal, J.; Omastova, M.; Fedorova, S.; Prokes, J.; Trchova, M. Polymer 2003, 44, 1353.
20. Moulton, S. E.; Innis, P. C.; Kane-Maguire, L. A. P.; Ngamna, O.; Wallace, G. G. Curr Appl Phys 2004, 4, 402.
21. Pink, Z.; Nauer, G. E.; Neugebauer, H.; Theiner, J.; Neckel, A. J Chem Soc Faraday Trans 1997, 93, 121.
22. Trchova, M.; Sapurina, I.; Prokes, J.; Stejskal, J. Synth Met 2003, 135/136, 305.
23. Dimitriev, O. P. Macromolecules 2004, 37, 3388.
24. Lu, X.; Ng, H. Y.; Xu, J.; He, C. Synth Met 2002, 128, 167.
25. Sakharov, I. Y.; Ouporov, I. V.; Vorobiev, A. K.; Roig, M. G.; Pletjushkina, O. Y. Synth Met 2004, 142, 127.
26. Behen, J. J.; Dwyer, R. F.; Bierl, B. A. Anal Biochem 1964, 9, 127.
27. Salaneck, W. R.; Leidberg, B.; Inganas, O.; Erlandsson, R.; Lundstrom, I.; MacDiarmid A. G.; Halpern, M.; Somasiri, N. L. D. Mol Cryst Liq Cryst 1985, 121, 191.
28. Zengin, H.; Zhou, W.; Jin, J.; Czerw, R.; Smith, D. W., Jr.; Echegoyen, L.; Carroll, D. L.; Foulger, S. H.; Ballato, J. Adv Mater 2002, 14, 1480.
29. Rao, P. S.; Anand, J.; Palaniappan, S.; Sathyanarayana, D. N. Eur Polym J 2000, 36, 915.
30. Gurunathan, K.; Trivedi, D. C. Mater Lett 2000, 45, 262.
31. Ryu, K. S.; Chang, S. H.; Kang, S. G.; Oh, E. J.; Yo, C. H. Bull Korean Chem Soc 1999, 20, 333.
32. Bae, W. J.; Jo, W. H.; Park, Y. H. Synth Met 2003, 132, 239.
33. Pouget, J. P.; Oblakowski, Z.; Nogami, Y.; Albouy, P. A.; Laridjani, M.; Oh, E. J.; Min, Y.; MacDiarmid, A. G.; Tsukamoto, J.; Ishiguro, T.; Epstein, A. J. Synth Met 1994, 65, 131.
34. Cao, Y.; Smith, P.; Heeger, A. J. Synth Met 1992, 48, 91.
35. Cao, Y.; Qiu, J. J.; Smith, P. Synth Met 1995, 69, 187.
36. Li W, Wan M. Synth Met 1998, 92, 121.
37. Chen, C. H. J Appl Polym Sci 2003, 89, 2142.
38. Molyneux, P. In Water: A Comprehensive Treatise; Franka, F., Ed.; Plenum: London, New York, 1975; Vol. 4, Chapter 7.